

# Self-sustained three-dimensional beating of a model eukaryotic flagellum

Bhargav Rallabandi<sup>1</sup>, Qixuan Wang<sup>2</sup>, and Mykhailo Potomkin<sup>2</sup>

<sup>1</sup>Department of Mechanical Engineering, University of California, Riverside, CA 92521, USA

<sup>2</sup>Department of Mathematics, University of California, Riverside, CA 92521, USA

## 1 Details of model derivation

We detail the derivation of the system (14) of the main text starting from equations (2)-(9).

Equations derived from the force balance. First, we recall the force balance for the flagellum (2a) of the main text for a point  $s$ , which we combine with local resistive force theory to write

$$\partial_s \mathbf{F} - \mathbf{R} \cdot \mathbf{v} = \mathbf{0}, \text{ where } \mathbf{R} = 8\pi\nu\xi_\perp \left( \mathbf{I} - \frac{\xi_\perp - \xi_\parallel}{\xi_\perp} \mathbf{d}\mathbf{d} \right). \quad (\text{S1})$$

The resistance matrix  $\mathbf{R}$  is invertible and  $\mathbf{R}^{-1} = \frac{1}{8\pi\nu\xi_\perp} \left( \mathbf{I} + \frac{\xi_\perp - \xi_\parallel}{\xi_\parallel} \mathbf{d}\mathbf{d} \right)$ , so one can rearrange (S1) as

$$\mathbf{v} = \mathbf{R}^{-1} (\partial_s \mathbf{F}). \quad (\text{S2})$$

Differentiating (S1), using  $\mathbf{v} = \int_0^s \partial_t \mathbf{d}(\tilde{s}, t) d\tilde{s}$  (which implies  $\partial_s \mathbf{v} = \partial_t \mathbf{d}$ ), and the identity (S2) lets us eliminate  $\mathbf{v}$  explicitly to yield

$$\partial_s^2 \mathbf{F} - (\partial_s \mathbf{R}) \cdot \mathbf{R}^{-1} (\partial_s \mathbf{F}) = \mathbf{R} \partial_t \mathbf{d}. \quad (\text{S3})$$

Next, we rewrite (S3) in basis  $\{\mathbf{e}_1, \mathbf{e}_2, \mathbf{d}\}$ . To this end, introduce the matrix  $\mathcal{P} = [\mathbf{e}_1 \ \mathbf{e}_2 \ \mathbf{d}]$ . Given a vector  $\mathbf{X}$ , we denote its coordinates in basis  $\{\mathbf{e}_1, \mathbf{e}_2, \mathbf{d}\}$  by  $\hat{X}$ , that is,  $\mathbf{X} = \mathcal{P}\hat{X}$ . It is useful to find  $\mathcal{P}'$  where  $'$  may denote the derivative either in  $t$  or in  $s$ :

$$\mathcal{P}' = \mathcal{P}\Omega, \text{ where } \Omega = \begin{pmatrix} 0 & -\phi'_3 & \phi'_2 \\ \phi'_3 & 0 & -\phi'_1 \\ -\phi'_2 & \phi'_1 & 0 \end{pmatrix}.$$

The matrix  $\Omega$  determines rotations, that is,  $\Omega\mathbf{X} = \boldsymbol{\omega} \times \mathbf{X}$  with  $\boldsymbol{\omega} = (\phi'_1, \phi'_2, \phi'_3)^\text{T}$ . For example, if  $\mathbf{H} := \partial_s \mathbf{F}$ , then  $\hat{H} = \partial_s \hat{F} + \Omega \hat{F}$  where  $\mathbf{H} = \mathcal{P}\hat{H}$  and  $\mathbf{F} = \mathcal{P}\hat{F}$ . Note also that  $\mathcal{P}^{-1} = \mathcal{P}^\text{T}$  and

$$\Lambda := \mathcal{P}^\text{T} (\partial_s \mathbf{R}) \mathbf{R}^{-1} \mathcal{P} = - \left( 1 - \frac{1}{\chi} \right) \begin{pmatrix} 0 & 0 & \chi\phi'_2 \\ 0 & 0 & -\chi\phi'_1 \\ \phi'_2 & -\phi'_1 & 0 \end{pmatrix}$$

$$\mathcal{P}^\text{T} \mathbf{R} \partial_t \mathbf{d} = \mathcal{P}^\text{T} \mathbf{R} \mathcal{P} \begin{bmatrix} \partial_t \phi_2 \\ -\partial_t \phi_1 \\ 0 \end{bmatrix} = 8\pi\nu\zeta_\perp \begin{bmatrix} \partial_t \phi_2 \\ -\partial_t \phi_1 \\ 0 \end{bmatrix} \quad (\text{Note that } \mathcal{P}^\text{T} \mathbf{R} \mathcal{P} \neq 8\pi\nu\zeta_\perp \mathbf{I}).$$

Applying  $\mathcal{P}^T$  to (S3) and using the equalities above we have

$$\partial_s \hat{H} + \Omega \hat{H} + \Lambda \hat{H} = 8\pi\nu\zeta_\perp \begin{bmatrix} \partial_t \phi_2 \\ -\partial_t \phi_1 \\ 0 \end{bmatrix}. \quad (\text{S4})$$

For  $\hat{H} = (H_1, H_2, H_3)^T$  and  $\hat{F} = (F_1, F_2, F_3)^T$  the equality  $\hat{H} = \partial_s \hat{F} + \Omega \hat{F}$  translates into

$$H_1 = F_1' - \phi_3' F_2 + \phi_2' F_3, \quad H_2 = F_2' + \phi_3' F_1 - \phi_1' F_3, \quad H_3 = F_3' + \phi_1' F_2 - \phi_2' F_1. \quad (\text{S5})$$

Here and below ' denotes the derivative specifically in variable  $s$ . Substituting (S5) into (S4) we obtain dimensional equations (14abc) of the main text.

Equations derived from the torque balance. Next, we derive equation (14def) of the main text from the torque balance:

$$\partial_s \mathbf{M}_{\text{bend}} + \partial_s \mathbf{M}_{\text{slide}} + \mathbf{d} \times \mathbf{F} + \mathbf{m}_v = 0. \quad (\text{S6})$$

The bending moment  $\mathbf{M}_{\text{bend}} = B_1 \phi_1' \mathbf{e}_1 + B_2 \phi_2' \mathbf{e}_2 + J \phi_3' \mathbf{d}$  can be written as

$$\mathbf{M}_{\text{bend}} = \mathcal{P} \begin{bmatrix} B_1 \phi_1' \\ B_2 \phi_2' \\ J \phi_3' \end{bmatrix},$$

Hence,

$$\partial_s \mathbf{M}_{\text{bend}} = \mathcal{P} \left[ \partial_s \hat{M}_{\text{bend}} + \Omega \hat{M}_{\text{bend}} \right] = \mathcal{P} \begin{bmatrix} B_1 \phi_1'' + (J - B_2) \phi_2' \phi_3' \\ B_2 \phi_2'' + (B_1 - J) \phi_1' \phi_3' \\ J \phi_3'' + (B_2 - B_1) \phi_1' \phi_2' \end{bmatrix}. \quad (\text{S7})$$

The sliding moment  $\mathbf{M}_{\text{slide}}$  is given by (see (7) in the main text)

$$\mathbf{M}_{\text{slide}} = \sum_{i=1}^N \mathbf{r}_i \times \mathbf{F}_{\text{slide}}, \quad \text{where } \mathbf{F}_{\text{slide}} = \int_s^L \mathbf{d}(u, t) f_i(u, t) du.$$

Recall that  $f_i(s, t)$  is the magnitude of the sliding force exerted by the  $(s, L)$  part on the  $[0, s]$ ,  $\mathbf{r}_i = a(\cos \theta_i \mathbf{e}_1 + \sin \theta_i \mathbf{e}_2)$  is the distance between the centerline and the  $i$ th microtubule doublet, and  $N = 9$  is the number of doublets. Then

$$\partial_s \mathbf{M}_{\text{slide}} = \sum_{i=1}^N [\partial_s \mathbf{r}_i \times \mathbf{F}_{\text{slide}} - f_i(\mathbf{r}_i \times \mathbf{d})].$$

Following [1, 2], we neglect the term  $\partial_s \mathbf{r}_i \times \mathbf{F}_{\text{slide}}$ . This assumption can be rationalized by the smallness of  $\phi_k'$  ( $k = 1, 2, 3$ ) and that the term  $\partial_s \mathbf{r}_i \times \mathbf{F}_{\text{slide}}$  is one order higher with respect to  $\phi_k'$  ( $k = 1, 2, 3$ ) than  $f_i(\mathbf{r}_i \times \mathbf{d})$  due to

$$\partial_s \mathbf{r}_i = a \phi_3' [-\sin \theta_i \mathbf{e}_1 + \cos \theta_i \mathbf{e}_2] + a(\phi_1' \sin \theta_i - \phi_2' \cos \theta_i) \mathbf{d}.$$

Due to this simplification and  $\mathbf{r}_i \times \mathbf{d} = a(\sin \theta_i \mathbf{e}_1 - \cos \theta_i \mathbf{e}_2)$  we write

$$\partial_s \mathbf{M}_{\text{slide}} = \mathcal{P} \begin{bmatrix} -a \sum_{i=1}^N f_i \sin \theta_i \\ a \sum_{i=1}^N f_i \cos \theta_i \\ 0 \end{bmatrix}. \quad (\text{S8})$$

Analogously, the term  $\mathbf{d} \times \mathbf{F}$  can be written as

$$\mathbf{d} \times \mathbf{F} = -F_2 \mathbf{e}_1 + F_1 \mathbf{e}_2 = \mathcal{P} \begin{bmatrix} -F_2 \\ F_1 \\ 0 \end{bmatrix}. \quad (\text{S9})$$

As it is written in the main text, following [3, page 49] the viscous moment  $\mathbf{m}_v$  is estimated as

$$\mathbf{m}_v = -2\pi a^2 \nu \partial_t \phi_3 \mathbf{d} = \mathcal{P} \begin{bmatrix} 0 \\ 0 \\ -2\pi a^2 \nu \partial_t \phi_3 \end{bmatrix}. \quad (\text{S10})$$

Applying  $\mathcal{P}^{-1}$  to the torque balance (S6) and using (S7), (S8), (S9), (S10), we get the system

$$\begin{cases} B_1 \phi_1'' + (J - B_2) \phi_2' \phi_3' - a \sum_{i=1}^N f_i \sin \theta_i - F_2 = 0, \\ B_2 \phi_2'' + (B_1 - J) \phi_1' \phi_3' + a \sum_{i=1}^N f_i \cos \theta_i + F_1 = 0, \\ J \phi_3'' + (B_2 - B_1) \phi_1' \phi_2' - 2\pi a^2 \nu \partial_t \phi_3 = 0. \end{cases} \quad (\text{S11})$$

In order to write terms  $a \sum_{i=1}^N f_i \sin \theta_i$  and  $a \sum_{i=1}^N f_i \cos \theta_i$  we introduce continuation in  $\theta_i$ .

Model continuous in  $\theta$ ; expression for  $f_i$ . We now homogenize the 9-filament structure by treating  $\theta$  as continuous. We recall expressions for  $f_i(s, t) = f(\theta_i, s, t)$  from the main text:

$$f_i = f_i^{\text{spr}} + f_i^{\text{mot}} = K(\Delta_{i-1} - 2\Delta_i + \Delta_{i+1}) - \rho(W_i n_i - W_{i-1} n_{i-1}) \quad (\text{S12})$$

Here  $\Delta_i = \Delta(\theta_i, s, t) = a(\phi_2(s, t) \cos \theta_i - \phi_1(s, t) \sin \theta_i)$  is the sliding displacement,  $\rho$  is the dynein motor mean number density,  $n_i(s, t) = n(\theta, s, t)$  is the fraction of the engaged motors, and  $W_i(s, t) = W(\theta, s, t)$  is the load of a motor on the  $i$ th filament given by (see expression for  $W_i$  (8) from the main text):

$$W(\theta, s, t) = \frac{F_0}{v_0} (v_0 - \partial_t (\Delta_{i+1} - \Delta_i)).$$

Assuming that all the functions  $\Delta$ ,  $W$ , and  $n$  are smooth and  $2\pi$ -periodic in  $\theta$  we can rewrite (S12) as

$$f = d\theta \left( \hat{K} \partial_\theta^2 \Delta - \rho \partial_\theta (W n) \right) \quad \text{and} \quad W(\theta, s, t) = \frac{F_0}{v_0} (v_0 + a d\theta (\partial_t \phi_2 \sin \theta + \partial_t \phi_1 \cos \theta)),$$

where  $\hat{K} = (d\theta)K$  and  $d\theta = 2\pi/N$ . Then we can rewrite terms  $a \sum_{i=1}^N f_i \sin \theta_i$  and  $a \sum_{i=1}^N f_i \cos \theta_i$  as

$$\begin{aligned}
a \sum_{i=1}^N f_i \sin \theta_i &\approx a \int_0^{2\pi} \left( \hat{K} \partial_\theta^2 \Delta - \rho \partial_\theta (Wn) \right) \sin \theta \, d\theta \\
&= -a \hat{K} \int_0^{2\pi} \Delta \sin \theta \, d\theta + a \rho \int_0^{2\pi} Wn \cos \theta \, d\theta \\
&= -a \hat{K} \int_0^{2\pi} (a(\phi_2 \cos \theta - \phi_1 \sin \theta)) \sin \theta \, d\theta \\
&\quad + \frac{a \rho F_0}{v_0} \int_0^{2\pi} \left( v_0 + \frac{2\pi a}{N} (\partial_t \phi_2 \sin \theta + \partial_t \phi_1 \cos \theta) \right) n \cos \theta \, d\theta \\
&= \pi a^2 \hat{K} \phi_1 + 2\pi a \rho F_0 \langle n \cos \theta \rangle + \frac{2\pi^2 a^2 \rho F_0}{N v_0} \partial_t \phi_2 \langle n \sin 2\theta \rangle + \frac{2\pi^2 a^2 \rho F_0}{N v_0} \partial_t \phi_1 (\langle n \cos 2\theta \rangle + \langle n \rangle).
\end{aligned}$$

Here  $\langle g \rangle$  denotes the average of  $g(\theta)$  in  $\theta$ :  $\langle g \rangle = \frac{1}{2\pi} \int_0^{2\pi} g(\theta) \, d\theta$ . Analogously, we obtain

$$a \sum_{i=1}^N f_i \cos \theta_i \approx -\pi a^2 \hat{K} \phi_2 - 2\pi a \rho F_0 \langle n \sin \theta \rangle - \frac{2\pi^2 a^2 \rho F_0}{N v_0} \partial_t \phi_2 (\langle n \rangle - \langle n \cos 2\theta \rangle) - \frac{2\pi^2 a^2 \rho F_0}{N v_0} \partial_t \phi_1 \langle n \sin 2\theta \rangle.$$

Now, introduce  $n_k^c$ ,  $n_k^s$ , and  $n_\pm^c$  as in (15) of the main text:

$$n_k^c = 2\langle n \cos(k\theta) \rangle, \quad n_k^s = 2\langle n \sin(k\theta) \rangle, \quad n_\pm^c = n_0^c \pm n_2^c.$$

With these notations we have

$$-a \sum_{i=1}^N f_i \sin \theta_i \approx -\frac{2\pi^2 a^2 K}{N} \phi_1 - \pi a \rho F_0 \left( n_1^c + \frac{\pi a}{N v_0} (n_+^c \partial_t \phi_1 + n_2^s \partial_t \phi_2) \right), \quad (\text{S13})$$

$$a \sum_{i=1}^N f_i \cos \theta_i \approx -\frac{2\pi^2 a^2 K}{N} \phi_1 - \pi a \rho F_0 \left( n_1^s + \frac{\pi a}{N v_0} (n_2^s \partial_t \phi_1 + n_-^c \partial_t \phi_2) \right). \quad (\text{S14})$$

Substituting (S13) and (S14) into (S11) we yields dimensional version of (14def). After non-dimensionalization based on Table 2 from the main text we obtain the system (14) of the main text.

## 2 Numerical solution of the model system

Here, we describe how we solve the model system

$$F_1'' - 2\phi_3'F_2' + (1 + \chi)\phi_2'F_3' - \left(\chi(\phi_2')^2 + (\phi_3')^2\right)F_1 + (\chi\phi_1'\phi_2' - \phi_3'')F_2 + (\phi_1'\phi_3' + \phi_2'')F_3 \quad (\text{S15a})$$

$$= \text{Sp}^4 \partial_t \phi_2 \quad (\text{S15b})$$

$$F_2'' + 2\phi_3'F_1' - (1 + \chi)\phi_1'F_3' + (\chi\phi_1'\phi_2' + \phi_3'')F_1 - \left(\chi(\phi_1')^2 + (\phi_3')^2\right)F_2 + (\phi_2'\phi_3' - \phi_1'')F_3 \quad (\text{S15c})$$

$$= -\text{Sp}^4 \partial_t \phi_1$$

$$F_3'' - \frac{1 + \chi}{\chi}\phi_2'F_1' + \frac{1 + \chi}{\chi}\phi_1'F_2' + \left(\frac{1}{\chi}\phi_1'\phi_3' - \phi_2''\right)F_1 + \left(\phi_1'' + \frac{1}{\chi}\phi_2'\phi_3'\right)F_2 - \frac{1}{\chi}\left((\phi_1')^2 + (\phi_2')^2\right)F_3 = 0 \quad (\text{S15d})$$

$$\mathcal{B}_1\phi_1'' - (\mathcal{B}_2 - \mathcal{J})\phi_2'\phi_3' - F_2 - \mu_K\phi_1 - \mu_a(n_1^c + \zeta(n_+^c\partial_t\phi_1 + n_2^s\partial_t\phi_2)) = 0 \quad (\text{S15e})$$

$$\mathcal{B}_2\phi_2'' + (\mathcal{B}_1 - \mathcal{J})\phi_1'\phi_3' + F_1 - \mu_K\phi_2 - \mu_a(n_1^s + \zeta(n_2^s\partial_t\phi_1 + n_-^c\partial_t\phi_2)) = 0 \quad (\text{S15f})$$

$$\mathcal{J}\phi_3'' + (\mathcal{B}_2 - \mathcal{B}_1)\phi_1'\phi_2' = \frac{\text{Sp}^4}{4\xi_\perp\Lambda^2}\partial_t\phi_3, \quad (\text{S15g})$$

$$\partial_t n = \beta(1 - n) - (1 - \beta)n \exp\{1 + 2\zeta(\partial_t\phi_1 \cos\theta + \partial_t\phi_2 \sin\theta)\} + \Lambda\mathcal{N}, \quad (\text{S15h})$$

where  $\mathcal{B}_1 = \mathcal{B} = B_1/B_2 \geq 1$ ,  $\mathcal{B}_2 = B_2/B_2 = 1$  and  $\mathcal{J} = J/B_2$  (filament made of a homogeneous linear elastic material has  $\mathcal{B} = 1$ ,  $\mathcal{J} = 2$ ). In the isotropic case  $\mathcal{B}_1 = 1$ ,  $\phi_3$  relaxes to zero exponentially on a time scale  $4\mathcal{J}\xi_\perp\Lambda^2/\text{Sp}^4$ .

*Solution strategy:* We mostly follow the computational strategy from [2]. Below we describe the  $(m + 1)$ th numerical step from  $(\phi_k^{(m)}, F_k^{(m)}, n^{(m)})$ ,  $k = 1, 2, 3$ , at time  $t = t_m$  to  $(\phi_k^{(m+1)}, F_k^{(m+1)}, n^{(m+1)})$ ,  $k = 1, 2, 3$ , at time  $t = t_{m+1}$ .

**STEP 1:** Solve (S15e) and (S15f) for  $\partial_t\phi_1$  and  $\partial_t\phi_2$ :

$$\left. \begin{aligned} \partial_t\phi_1 &= \frac{1}{A}(n_-^c G_1 - n_2^s G_2), \\ \partial_t\phi_2 &= \frac{1}{A}(n_+^c G_2 - n_2^s G_1), \end{aligned} \right\} \quad (\text{S16})$$

where  $A = n_+^c n_-^c - (n_2^s)^2$  and

$$\begin{aligned} G_1 &= (\zeta\mu_a)^{-1} [\mathcal{B}_1\phi_1'' - (\mathcal{B}_2 - \mathcal{J})\phi_2'\phi_3' - F_2 - \mu_K\phi_1 - \mu_a n_1^c], \\ G_2 &= (\zeta\mu_a)^{-1} [\mathcal{B}_2\phi_2'' + (\mathcal{B}_1 - \mathcal{J})\phi_1'\phi_3' + F_1 - \mu_K\phi_2 - \mu_a n_1^s]. \end{aligned}$$

**STEP 2:** Update  $F_k$ , that is, calculate  $F_k^{(m+1)}$ ,  $k = 1, 2, 3$ . To this end, substitute (S16), with  $G_j$ ,  $j = 1, 2$ ,  $n_\pm^c$ ,  $n_2^s$ , calculated using values at the previous time step  $t = t_m$ , into (S15a) and (S15c). One obtains the system of three linear elliptic equations for  $F_1^{(m+1)}$ ,  $F_2^{(m+1)}$ ,  $F_3^{(m+1)}$ . This system is written below; all super-indexes indicating the time step are dropped to make notations concise: values of  $A$ ,  $\phi_1$ ,  $\phi_2$ ,  $\phi_3$ ,  $n_\pm^c$ ,  $n_2^s$  are taken from the  $m$ th step, whereas values of  $F_1$ ,  $F_2$ ,  $F_3$  are from the  $m + 1$  step,

and the system is solved numerically for  $F_1, F_2, F_3$ .

$$\begin{aligned}
& AF_1'' - 2A\phi_3'F_2' + (1 + \chi)A\phi_2'F_3' - \left( A \left( \chi (\phi_2')^2 + (\phi_3')^2 \right) + \frac{n_+^c \text{Sp}^4}{\zeta\mu_a} \right) F_1 \\
& + \left( A (\chi\phi_1'\phi_2' - \phi_3'') - \frac{n_2^s \text{Sp}^4}{\zeta\mu_a} \right) F_2 + A (\phi_2'' + \phi_1'\phi_3') F_3 \\
& = -\frac{\text{Sp}^4}{\zeta\mu_a} \left\{ \mathcal{B}_1 n_2^s \phi_1'' - \mathcal{B}_2 n_+^c \phi_2'' - (\mathcal{B}_2 - \mathcal{J}) n_2^s \phi_2' \phi_3' - (\mathcal{B}_1 - \mathcal{J}) n_+^c \phi_1' \phi_3' \right. \\
& \quad \left. - \mu_K (n_2^s \phi_1 - n_+^c \phi_2) - \mu_a (n_2^s \hat{n}_1^c - n_+^c \hat{n}_1^s) \right\} \tag{S17a}
\end{aligned}$$

$$\begin{aligned}
& AF_2'' + 2A\phi_3'F_1' - (1 + \chi)A\phi_1'F_3' + \left( A (\chi\phi_1'\phi_2' + \phi_3'') - \frac{n_2^s \text{Sp}^4}{\zeta\mu_a} \right) F_1 \\
& - \left( A \left( \chi (\phi_1')^2 + (\phi_3')^2 \right) + \frac{n_-^c \text{Sp}^4}{\zeta\mu_a} \right) F_2 - A (\phi_1'' - \phi_2'\phi_3') F_3 \\
& = -\frac{\text{Sp}^4}{\zeta\mu_a} \left\{ \mathcal{B}_1 n_-^c \phi_1'' - \mathcal{B}_2 n_2^s \phi_2'' - (\mathcal{B}_2 - \mathcal{J}) n_-^c \phi_2' \phi_3' - (\mathcal{B}_1 - \mathcal{J}) n_2^s \phi_1' \phi_3' \right. \\
& \quad \left. - \mu_K (n_-^c \phi_1 - n_2^s \phi_2) - \mu_a (n_-^c \hat{n}_1^c - n_2^s \hat{n}_1^s) \right\} \tag{S17b}
\end{aligned}$$

$$\begin{aligned}
& F_3'' - \frac{1 + \chi}{\chi} \phi_2' F_1' + \frac{1 + \chi}{\chi} \phi_1' F_2' + \left( \frac{1}{\chi} \phi_1' \phi_3' - \phi_2'' \right) F_1 + \left( \phi_1'' + \frac{1}{\chi} \phi_2' \phi_3' \right) F_2 \\
& - \frac{1}{\chi} \left( (\phi_1')^2 + (\phi_2')^2 \right) F_3 = 0. \tag{S17c}
\end{aligned}$$

**STEP 3:** Update  $\phi_k$ , that is, calculate  $\phi_k^{(m+1)}$ ,  $k = 1, 2, 3$ . This can be done by using the following system composed of (S15a), (S15c), and (S15g):

$$\partial_t \begin{pmatrix} \phi_1 \\ \phi_2 \\ \phi_3 \end{pmatrix} = \frac{1}{\text{Sp}^4} \begin{pmatrix} F_3 \phi_1'' - F_1 \phi_3'' + (1 + \chi) F_3' \phi_1' - 2 F_1' \phi_3' + \chi F_2 (\phi_1')^2 + F_2 (\phi_3')^2 \\ \quad - \chi F_1 \phi_1' \phi_2' - F_3 \phi_2' \phi_3' - F_2'' \\ F_3 \phi_2'' - F_2 \phi_3'' + (1 + \chi) F_3' \phi_2' - 2 F_2' \phi_3' - \chi F_1 (\phi_2')^2 - F_1 (\phi_3')^2 \\ \quad + \chi F_2 \phi_1' \phi_2' + F_3 \phi_1' \phi_3' + F_1'' \\ 4\xi_{\perp} \Lambda^2 \{ \mathcal{J} \phi_3'' + (\mathcal{B}_2 - \mathcal{B}_1) \phi_1' \phi_2' \} \end{pmatrix}$$

Values of  $F_k$  are taken from STEP 2.

**STEP 4:** Finally, update fraction of engaged motors  $n$  by numerical integration of (S15h); values of  $\partial_t \phi_1$  and  $\partial_t \phi_2$  are taken from STEP 1.

### 3 Sensitivity to initial conditions

We study the sensitivity of the solutions to initial conditions. This is done by running the simulation starting from time  $t = 0$  with an initially straight flagellum as described in the main text. However, we now we apply an additional force to the tip of the flagellum, directed along the axis of the undeformed flagellum ( $\mathbf{e}_y$ ) over an initial duration  $0 < t < t_{\text{init}}$ . This condition can be expressed as  $\mathbf{F}(s = 1, 0 < t < t_{\text{init}}) = F_{\text{tip}} \mathbf{e}_y$ , where  $F_{\text{tip}} > 0$  puts the flagellum under tension while  $F_{\text{tip}} < 0$  puts it under compression. At the end of this time interval, we set  $F_{\text{tip}} = 0$ , and the simulation thereafter continues

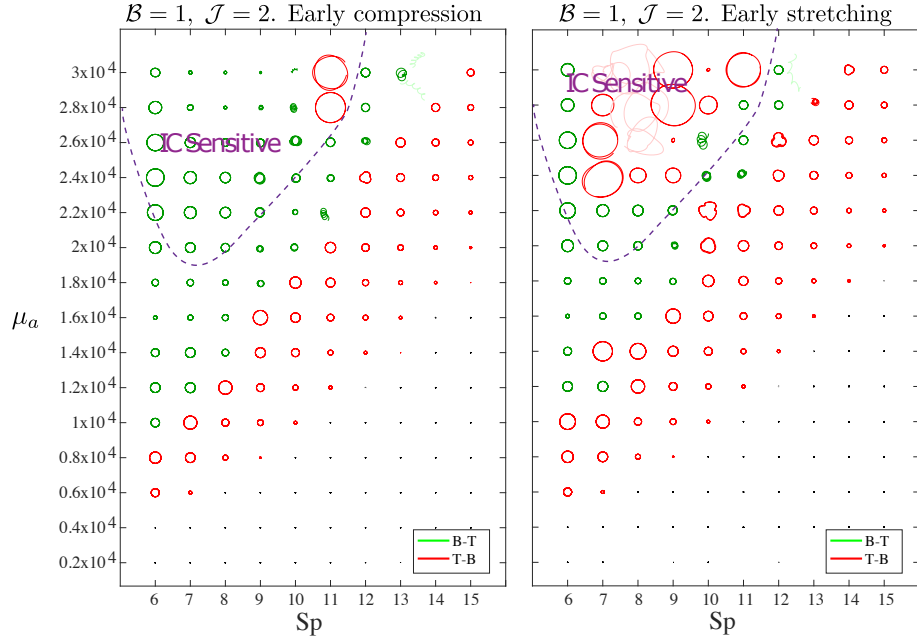


**Figure S1: Sensitivity to initial conditions of an isotropic flagellum** ( $\mathcal{B} = 1$ ,  $\mathcal{J} = 2$ ) under an initial compression (left) or stretch (right). Plotted trajectories correspond to long times after transients have decayed. The trajectories are quantitatively independent of initial conditions except in the “IC sensitive” region corresponding to large motor activity and small  $Sp$ . Slight sensitivity to initial conditions also occurs around the transition from retrograde to anterograde wave propagation. All notations are the same as in Figure 5 from the main text.

to run according to the governing equations and boundary conditions described in the main text (in particular the free end of the flagellum becomes force-free for  $t > t_{\text{init}}$ ). The effect of this procedure is to prepare the state of the flagellum over a duration  $t_{\text{init}}$  in a way that is biased by the applied tip force.

We use  $t_{\text{init}} = 15$  and  $F_{\text{tip}} = \pm Sp^2/2$  (note that the forces in the problem scale as  $Sp^2$  as predicted by linear stability analysis) and run the simulations until beating patterns appear stable (typically  $t \gtrsim 150$ ). Over most of the phase space, the initial preparation with the tip force does not affect the final beating state of the flagellum. However, in the region of the  $Sp - \mu_a$  phase plane marked as “IC-sensitive”, the emergent beating patterns depend on how the flagellum is initially prepared. In particular, when the flagellum is prepared with an initial compression, the beating patterns at long times tend to show anterograde wave propagation. By contrast, preparing the flagellum with an initial stretch appears to encourage trajectories with retrograde waves. Some sensitivity to initial conditions also occurs near the threshold between retrograde and anterograde wave behaviors. Across the rest of the phase space, the beating patterns obtained are quantitatively identical independent of the initial preparation of the flagellum (Fig. S1 and Fig. 4 of the main text).

## 4 Results of numerical simulations for various twist moduli $\mathcal{J}$

We consider the effect of the twist modulus  $\mathcal{J}$  on the flagellum beating dynamics. The phase diagram in the  $Sp - \mu_a$  plane with  $\mathcal{B} = B_1/B_2 = 2$ ,  $\mathcal{J} = 2, 5, 10, 50$  are shown in Figure S2. As  $\mathcal{J}$  increases, the

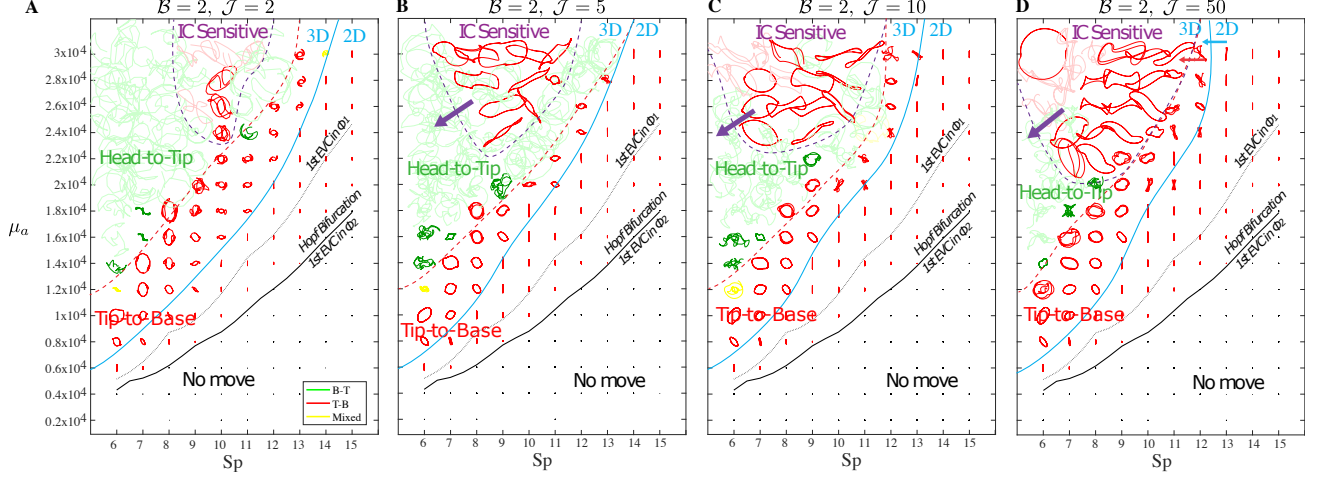


**Figure S2: Phase diagram for anisotropic flagellum with  $B_1/B_2 = 2$ ,  $J = 2, 5, 10, 50$ .** All notations are the same as in Figure 5 from the main text.

IC sensitive domain expands (Figure S2, purple arrows). The location of the Hopf bifurcation does not change as it is independent of both  $B$  and  $J$ . The 2D-to-3D transition threshold (Figure S2, blue solid curves) and the retrograde-to-antegrade transition threshold (Figure S2, red dashed curves) does not change much either, except at very large  $J = 50$  for which these curves move slightly to the left at large  $\mu_a$  values (Figure S2D). This resulting in a slight expansion of the domain of 2D beating, as well as the domain of beating with retrograde wave propagation. Together, our simulations show that the twist stiffness  $J$  plays a less important role than bending stiffness in regulating the beating patterns.

## 5 Approximate analysis of eigenvalue problem

In this section, we analyze the eigenvalue problem of section 3.2 of the main text and justify the approximate expression (27) for the threshold value of  $\mu_a$  for the onset of instability. The characteristic equation of (20b) governing the linearized dynamics of  $\phi_2$ ,  $(p^{(2)})^4 - \Phi(p^{(2)})^2 + Sp^4\sigma = 0$  admits solutions

$$p_1^{(2)} = -p_3^{(2)} = \sqrt{\frac{\Phi + \sqrt{\Phi^2 - 4Sp^4\sigma}}{2}}, \quad p_2^{(2)} = -p_4^{(2)} = \sqrt{\frac{\Phi - \sqrt{\Phi^2 - 4Sp^4\sigma}}{2}}. \quad (\text{S18})$$

The eigenvalue problem is solved by  $\det \mathcal{P}^{(\ell)} = 0$ . Substituting the above relations for  $p_i^{(2)}$  yields (equation (24) from the main text)

$$\Phi^2 - \Phi q^{(1)} q^{(2)} \tanh q^{(1)} \tanh q^{(2)} - 2\bar{\sigma}_1 \left(1 + \text{sech } q^{(1)} \text{sech } q^{(2)}\right) = 0, \quad (\text{S19})$$

which is so far exact.

Seeking solutions for which the  $p_{1,2}^{(2)}$  have large real parts lets us approximate  $\tanh p_1^{(2)} \tanh p_2^{(2)} \approx 1$ ,  $\text{sech } p_1^{(2)} \text{sech } p_2^{(2)} \ll 1$ . This reduces (S19) to the condition

$$\Phi^2 - \Phi p_1^{(2)} p_2^{(2)} - 2Sp^2\sigma \approx 0. \quad (\text{S20})$$

Now, there are several possibilities depending on the locations of  $p_1^{(2)}$  and  $p_2^{(2)}$  in the complex plane. If we assume  $0 < \arg(p_1^{(2)}) + \arg(p_2^{(2)}) < \pi$ , then (S18) yields  $p_1^{(2)} p_2^{(2)} = Sp^2\sqrt{\sigma}$ . Solving (S20) yields

$\Phi = -\text{Sp}^2\sqrt{\sigma}$  or  $\Phi = 2\text{Sp}^2\sqrt{\sigma}$ . The latter solution corresponds to repeated roots for  $p_i^{(2)}$  which is degenerate and we thus reject. The former solution,  $\Phi = -\text{Sp}\sqrt{\sigma}$ , (S18) yields

$$p_1^{(2)} = \text{Sp}\sqrt{\frac{(-1 + i\sqrt{3})\sqrt{\sigma}}{2}}, \quad p_2^{(2)} = \text{Sp}\sqrt{\frac{(-1 - i\sqrt{3})\sqrt{\sigma}}{2}}, \quad \Phi = -\text{Sp}^2\sqrt{\sigma} \quad (\text{S21})$$

Self-consistency with condition  $0 < \arg(p_1^{(2)}) + \arg(p_2^{(2)}) < \pi$  assumed above requires that  $|\arg(\sigma_1)| < 2\pi/3$ , which we find to be ultimately borne out by numerical solutions. Alternatively, if one assumes  $\pi < \arg(p_1^{(2)}) + \arg(p_2^{(2)}) < 2\pi$ , then (S18) yields  $p_1^{(2)}p_2^{(2)} = -\text{Sp}^2\sqrt{\sigma}$ . In this case the same analysis shows that the solutions of (S20) are either degenerate or are inconsistent with the above assumptions.

Thus, we accept (S21) and use  $\Phi = -\text{Sp}^2\sqrt{\sigma}$  in (21) of the main text to obtain

$$\Phi = \mu_K + \frac{2\mu_a\beta\zeta}{\Gamma}\sigma\left(1 - \left(1 - \frac{\beta}{\Gamma}\right)\frac{\alpha\Gamma}{\sigma + \Gamma}\right) \approx -\text{Sp}^2\sqrt{\sigma} \quad (\text{S22})$$

Numerical solutions of the approximate equation (S22) for typical parameters yield a single conjugate pair of complex growth rate  $\sigma$  that indeed satisfies all the above assumptions.

Stability threshold of the large- $\text{Re } p_i^{(2)}$  eigenmodes. We first rearrange (S22) by introducing the rescaled complex growth rate  $\lambda = \sigma/\Gamma$  (note that  $\Gamma$  is real) to obtain

$$\lambda\left(1 - \frac{\gamma}{1 + \lambda}\right) + \mathcal{K} = -\mathcal{G}\sqrt{\lambda}, \quad \text{where} \quad \mathcal{K} \equiv \frac{\mu_K}{2\mu_a\beta\zeta}, \quad \mathcal{G} \equiv \frac{\text{Sp}^2\Gamma^{1/2}}{2\mu_a\beta\zeta}, \quad \gamma = \alpha\left(1 - \frac{\beta}{\Gamma}\right). \quad (\text{S23})$$

The onset of instability of these modes correspond to the growth rate  $\lambda$  being imaginary, so we substitute  $\lambda = i\omega$  and separate real and imaginary parts to get

$$\frac{\mathcal{G}\sqrt{\omega}}{\sqrt{2}} + \mathcal{K} - \frac{\gamma\omega^2}{\omega^2 + 1} = \frac{\mathcal{G}\sqrt{\omega}}{\sqrt{2}} - \frac{\gamma\omega}{\omega^2 + 1} + \omega = 0,$$

The goal is to solve this for the mode oscillation frequency  $\omega$  and find a relation between  $\mathcal{G}$ ,  $\mathcal{K}$  and  $\gamma$  at which this frequency occurs.

We first rearrange the above for  $K$  and  $G$  in terms of  $\omega$  to obtain (26a) of the main text, which we repeat here

$$\frac{\mu_K}{2\mu_a\beta\zeta} = \mathcal{K}(\omega) = \frac{\omega(\gamma\omega - \gamma + \omega^2 + 1)}{\omega^2 + 1}, \quad \text{and} \quad \frac{\text{Sp}^2\Gamma^{1/2}}{2\mu_a\beta\zeta} = \mathcal{G}(\omega) = \frac{\sqrt{2\omega}(\gamma - \omega^2 - 1)}{\omega^2 + 1}. \quad (\text{S24})$$

This defines a parametric curve in  $\mathcal{K}$ - $\mathcal{G}$  space in terms of the parameter  $\omega$ . To obtain an explicit approximation of this curve, we recognize that because  $\mathcal{K}$  and  $\mathcal{G}$  are positive,  $\omega$  must lie in the range  $\omega_0 < \omega < \omega_1$ , where  $\omega_0 = \frac{1}{2}\left(\sqrt{\gamma^2 + 4\gamma - 4} - \gamma\right)$  corresponds to  $\mathcal{K} = 0$  and  $\omega_1 = \sqrt{\gamma - 1}$  corresponds to  $\mathcal{G} = 0$ . We now construct two-point linear approximations that are exact at both limits  $\omega = \omega_0$  and  $\omega = \omega_1$ . This gives

$$\begin{aligned} \mathcal{K} &\approx \mathcal{K}_1 \frac{\omega - \omega_0}{\omega_1 - \omega_0}, \quad \mathcal{G} \approx \mathcal{G}_0 \frac{\omega - \omega_1}{\omega_0 - \omega_1}, \quad \text{with} \\ \mathcal{K}_1 = \mathcal{K}(\omega_1) &= \frac{\omega_1(\gamma\omega_1 - \gamma + \omega_1^2 + 1)}{\omega_1^2 + 1}, \quad \mathcal{G}_0 = \mathcal{G}(\omega_0) = \frac{\sqrt{2\omega_0}(\gamma - \omega_0^2 - 1)}{\omega_0^2 + 1}. \end{aligned} \quad (\text{S25})$$

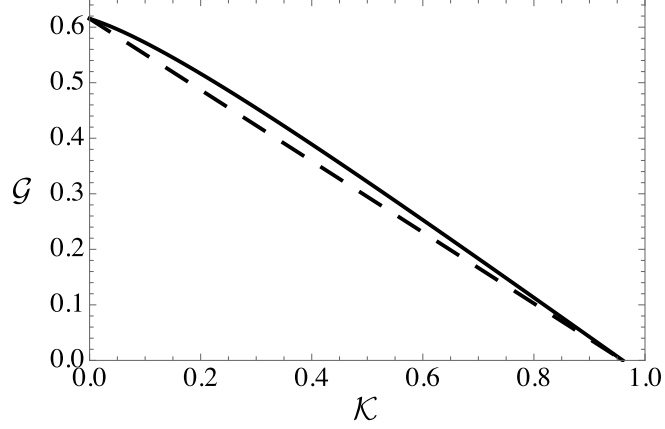


**Figure S3:** Stability threshold curve in  $\mathcal{K}$ - $\mathcal{G}$  space for a typical value of  $\gamma = 1.96$ , showing the parametric curve (S24) (solid) and its two-point linear approximation (S25) (dashed).

The parameter  $\omega$  is now easily eliminated to obtain the linear approximation

$$\mathcal{K} \approx C - D\mathcal{G}, \quad \text{where } C = \gamma - 1, \quad D = \frac{(\gamma - 1) \left( \gamma + 2 - \sqrt{\gamma^2 + 4\gamma - 4} \right)}{\left( \sqrt{\gamma^2 + 4\gamma - 4} - \gamma \right)^{3/2}}. \quad (\text{S26})$$

This approximation provides a good global approximation of the “exact” parametric curve (S24), as seen in Fig. S3. Equation (S26) can be cast in terms of  $\mu_a$ ,  $\mu_a$  and Sp to obtain (27) of the main text, which correctly captures the global stability behavior of the system.

## 6 Simulation videos

**Supplementary video 1:** Simulation of isotropic flagellum beating with  $\mathcal{B} = 1$ ,  $\mathcal{J} = 2$ , Sp = 10,  $\mu_a = 1.6 \times 10^4$ .

**Supplementary video 2:** Simulation of isotropic flagellum beating with  $\mathcal{B} = 1$ ,  $\mathcal{J} = 2$ , Sp = 7,  $\mu_a = 1.4 \times 10^4$ .

**Supplementary video 3:** Simulation of anisotropic flagellum beating with  $\mathcal{B} = 2$ ,  $\mathcal{J} = 5$ , Sp = 10,  $\mu_a = 1.6 \times 10^4$ .

**Supplementary video 4:** Simulation of anisotropic flagellum beating with  $\mathcal{B} = 2$ ,  $\mathcal{J} = 5$ , Sp = 8,  $\mu_a = 1.4 \times 10^4$ .

**Supplementary video 5:** Simulation of anisotropic flagellum beating with  $\mathcal{B} = 2$ ,  $\mathcal{J} = 5$ , Sp = 7,  $\mu_a = 1.6 \times 10^4$ .

## References

- [1] Oriola D, Gad lha H, Casademunt J. Nonlinear amplitude dynamics in flagellar beating. Royal Society Open Science. 2017;4(3):160698.

- [2] Chakrabarti B, Saintillan D. Spontaneous oscillations, beating patterns, and hydrodynamics of active microfilaments. *Physical Review Fluids*. 2019;4(4):043102.
- [3] Childress S. *Mechanics of Swimming and Flying*. vol. 2. Cambridge University Press; 1981.